2004:158 CIV

EXAMENSARBETE

Model Test of an Efficient Fish Lock as an Entrance to Fish Ladders at Hydropower Plants

Elianne Wassvik

MASTER OF SCIENCE PROGRAMME
Department of Applied Physics and Mechanical Engineering
Division of Fluid Mechanics

LULEÅ TEKNISKA UNIVERSITET

2004:158 CIV • ISSN: 1402 - 1617 • ISRN: LTU - EX - - 04/158 - - SE

Preface

This project has been carried out at the Division of Fluid Mechanics, Luleå University of Technology, Sweden, August 2003-May 2004. The supervisors for this project have been Professor Håkan Gustavsson and Dr Fredrik Engström. It is carried out as a Master Thesis for the Master of Science Program in Mechanical Engineering with focus towards Applied Mechanics. It has also been a part of the Research Trainee Program 2003-2004 at Luleå University of Technology.

Acknowledgements

I would like to thank my supervisors Professor Håkan Gustavsson and Dr Fredrik Engström for their support during this work. I would also like to thank technician Allan Holmgren for building and rebuilding the laboratory setup. A special thanks goes to my eleven Research Trainee colleagues for constant feedback and a stimulating working environment.

Luleå, May 2004
Elianne Wassvik

Abstract

Migrating fish that swim upstream in rivers for reproduction need to overcome obstructions, such as hydropower plants. If a fishway is used to help the fish pass such an obstacle, water needs to be taken from the dam without first passing through the turbines. Also, the fish may have difficulties finding the fishway, due to the dominating flow from the turbine tailrace.

A fish lock that uses turbine tailwater to entice the fish into the lock and further on to a fishway is studied. The fish lock is a shallow open channel that uses a small fraction of the tailwater. A local acceleration of the flow is created by changing the cross sectional area of the lock channel.

Measurements are concentrated on how to design the lock so enough water passes through and a sufficient velocity increment is reached. This is investigated in a lab-scale model using laser Doppler velocimetry. A full-scale prototype will then be tested at the Sikfors hydropower plant in the Pite river in Sweden.

Contents

1 Introduction

Fishways and fish locks are used to create a passage for migrating fish at obstructions in their path to or from their spawning ground. One such obstruction is hydropower plants, where the water for fishways or locks is usually taken from the dam without first passing through the turbines. Thus, this water can not be used to generate electricity. Another problem is that the fish have problem finding the entrance to the fishway or fish lock due to the dominating flow from the turbine tailrace.

The principle of the present fish lock is to operate without any water directly from the dam, using only water from the turbine tailrace, thus reducing the amount of water taken from the dam without passing the turbines. The lock is based on an idea from innovator Jan-Erik Almqvist, Boden, Sweden and is an open channel that will be partly submerged in the turbine tailrace so that water can flow through, and around it. At the entrance (downstream in the lock) a bump will reduce the cross sectional area of the lock, creating an increased speed at this point, which will attract the fish.

The fish lock will work as an entrance and a subsequent project will deal with the transport from the lock to the dam. The current project concentrates on finding how the highest speed increase of the water at the entrance is reached, by studying the flow in a model of the fish lock in lab-scale.

Steady 2-d flow over submerged bodies is a well studied area. However, the focus has been on wave phenomena. For instance, the wave generation of a submerged semicircular body has been studied by Forbes and Schwartz [1] and Vanden-Broeck [2]. Wave generation over other shapes has been studied by Faltas et al. [3] and Hanna [4].

The performance of the lock is compared with classic inviscid 2-d theory, where a bump that causes critical flow over it, will also create the highest velocity increase. In this case, where the fish lock only covers a small area of the tailrace, no damming of the water surface can occur. Instead, the flow rate will decrease inside the fish lock. An extended 2-d theory is developed, which takes the blockage effect in consideration and compares the velocity out of the lock with the velocity of the water around the lock.

The entrance speed to the lock must be related to the fish swimming capacity. The recommended speed at the entrance is 1.2 m/s for pacific salmon [5]. The fish lock in this project will be tested at the Sikfors hydropower plant (40 MW) in the Pite river in Sweden and the fish in that river, that use fish passages, are mainly salmon and salmon trout.

Fish swimming speed is categorized in three speeds; cruising, sustained and burst speed [5]. It is important that the flow speed at the entrance is as high as possible, compared to the surrounding flow speed, in order for the fish to find it without being higher than the fish's burst speed.

The salmon is very sensitive to differences in temperature[6] and pressure[7]. It is also nearsighted, so to navigate in poor visibility it uses ”distant touch“[8] which is a kind of radar system detecting small pressure variations in the water.

This thesis starts by describing the salmon life cycle and physique (if needed use glossary on page 41) and the most commonly used fishways and fish locks. Then tow-dimensional theory of flow over a bump is described and extended to fit the fish lock followed by the experimental setup of the model fish lock and results.

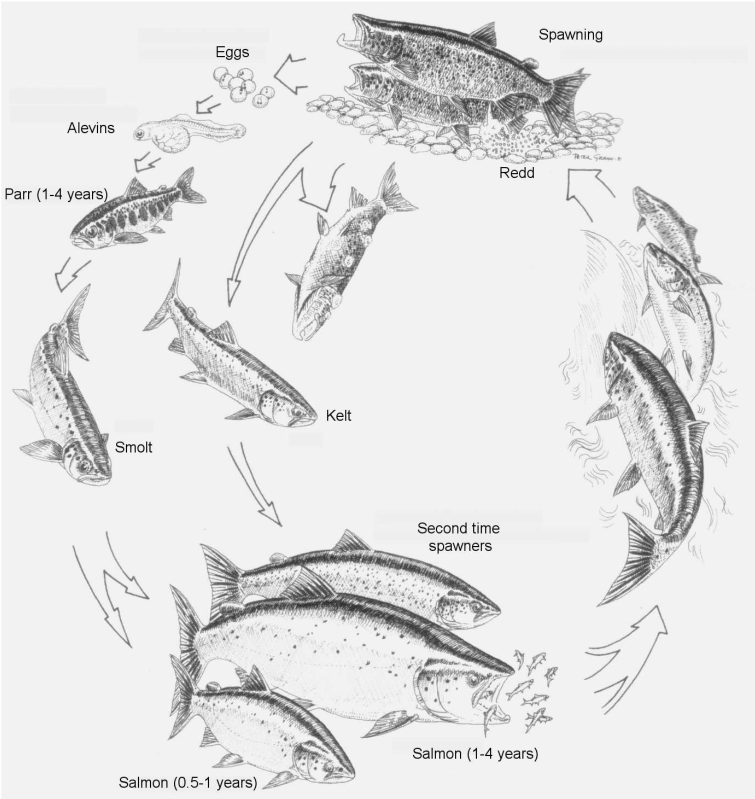

Figure 1: Life cycle of the salmon [10].

2 Salmon-like fishes

2.1 Life cycle

Salmon are anadromous fish, which means they reproduce in fresh water and live the rest of their life in salt water. The life cycle of the salmon can be categorized in four stages: spawning, life in fresh water, smoltification and life in salt water; see Figure 1 [9].

2.1.1 Spawning

When the salmon has spent 1-3 years maturing in the sea it returns to the home river for reproduction (the amount of salmon that swim to the wrong river is 1-2 %). In the Baltic sea the ascent to the river starts in April-June and in the Atlantic it starts in October the year before. To find the right river the salmon uses two orientation

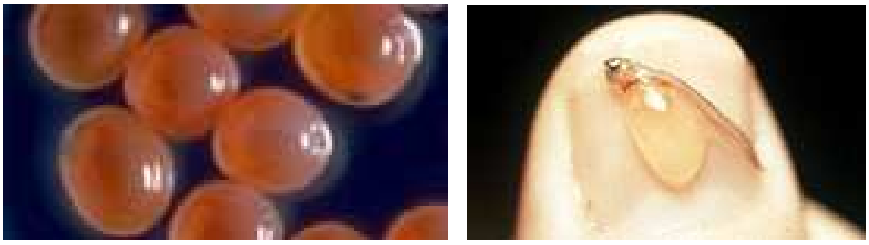

(a) Eyed-out salmon eggs [11]. (b) Salmon alevin with yolk sac [12].

Figure 2: Salmon eggs and newly hatched salmon (alevin).

techniques; in the sea it navigates using the sun and the earth magnetism, and when the salmon reaches the coast it tastes and smells the water to find the right river. [9]

The start of the salmon ascent in the river varies from river to river and from year to year. High flow rate makes the salmon arrive early and also brings a greater number of salmon than other years [9]. Even the water temperature has an effect on when the salmon arrives [10].

At the beginning of the season, big salmon with the most years in the sea arrive. Then comes the salmon with two years in the sea. This salmon has a mean weight of 7 kg. After this comes salmon that has spent one year in the sea and weighs between 1.5 and 3 kg. At last, in the late summer comes the big female salmon.[9]

During the ascent in the river the salmon changes. In order to avoid high content of lactic acid in the body, the salmon almost completely stops feeding when swiming up a river. After a week in the river the salmon changes its appearance. From being a silver shining fish, it gets a black brownish color and the male develops a hook in the lower jaw. [9]

The place for the redd (the nest) must fulfil two important criteria: the river bottom must be of stone and gravel with a diameter varying from 0.5 to 4 cm and through the redd water must flow with high content of oxygen. Most of the redds is at a water depth of 0.3 to 3 m. [9]

The spawning is in progress for a couple of weeks. The female salmon carries approximately 1000 eggs per kg body weight and lays approximately 200 eggs in each redd. [9]

After spawning, the salmon are called kelts and they either return directly to the sea or stay in the river until the water temperature reaches +8 °C [9]. Many of the salmon die because of the stress during the spawn and only 2 % of the salmon return to spawn a second time (10 % of the trout). [10]

2.1.2 Life in fresh water

The fry hatches after 410 degree-days (the mean temperature in Celsius in a day multiplied with the number of days). After 200 degree-days the egg becomes eyed-out, i.e. the eyes of the fetus are visible through the egg; see Figure 2(a). The nervous system is now almost fully developed. When the spawn is eyed-out it is very unsensitive and can even be sent by mail. [9]

After hatching, the fry stays in the redd (90 % of the fertilized eggs develop to hatching) [9]. During this time the fry is called alevins, and it feeds on the nourishment in a food sac attached to them (yolk sac); see Figure 2(b). The nourishment in the yolk sac gives the alevins food for about 180 degree-days, typically six weeks, and the fry is now 1.5 cm long [10].

After the nourishment in the yolk sac is gone, the fry is called parr. The parr feeds on small animals in the water. The limit for how much parr a river can produce depends on different factors such as flow rate, territory opportunity, production of nutrient, the competition for nutrient, number of enemies, climate and water quality. As an example, the Mörrumsån in southern Sweden can produce one smolt per m^2 and the Torne river in the northern Sweden can produce one smolt per 200 m^2. The fry is parr in one year in southern Sweden and three to four years in northern Sweden. [9]

2.1.3 Smoltification

When the parr reaches a size of 15 cm ($\pm$ 4 cm) it becomes smolt. This transformation takes place during a couple of weeks in April-May. The river the salmon smoltificates in is the river it returns to when spawning. During the smoltification the fry changes color from a greenish color to a silvery color and the smolt now gets the ability to live in saltwater. [9]

The smolt starts its descent to the sea when the water temperature reaches +10°C, and it descends with a speed of 0.5-2 km/day [10]. During the descent the smolt is exposed to predators and even though the smolt form schools, as much as 40 % can fall victim to predators [9].

When the smolt reaches the sea and starts the migration to the growth areas it is called postsmolt until it reaches a length of 25 cm [10]. There are mainly two growth areas for Swedish salmon. The west coast salmon has its growth areas around Island, Greenland and the Faroe Islands and the east coast salmon has its growth areas south and east of Gotland. In the sea, the access of food increases and there are more predators. After the first summer only 20 % of the emigrated smolt have survived. [9]

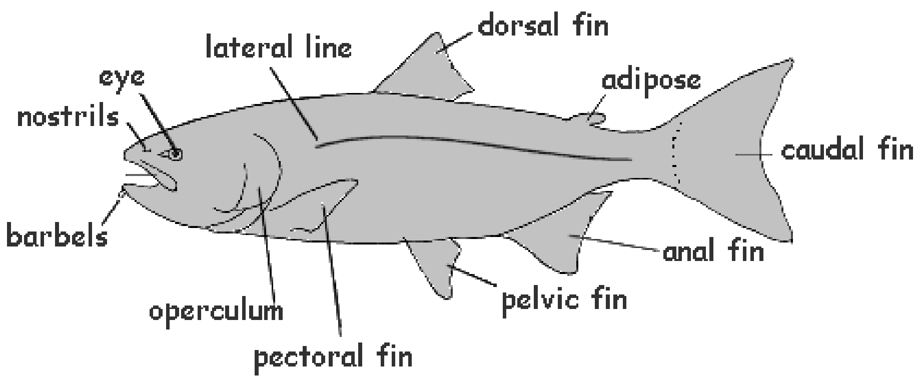

Figure 3: Fish anatomy [14].

2.1.4 Life in salt water

When the postsmolt reaches 25 cm it begins to eat small fish and will now grow rapidly. The best growth is in temperatures between 16-19 °C [13]. Already after a year, some of the salmon return to the home river for spawning. The salmon weighs after one year in the sea 1.5 to 3 kg. At the east coast, it is almost only males that return after one year. At the west coast, the amount of females is the same as the amount of males. [9]

Most of the salmon stay in the sea two to three years and sometimes even longer. In winter the salmon is at a depth of 75-100 m, but in the summer they are much closer to the surface (at night as close as 5 m). A salmon that spent two years in the sea weighs approximately 7 kg and a salmon that has spent three years in the sea weighs 15 kg, or more. 10-12 % of the emigrated salmon returns for spawning (somewhat lower for east coast salmon due to the pressure from fishing)[10].[9]

2.2 The salmons senses

2.2.1 Sight

As an adaption to the environment, the salmon is nearsighted, due to the poor visibility in water. The salmon has the sight of a predator which means it cannot see static objects very well. It can see colors, but only in daylight. [7]

2.2.2 Hearing

The salmon ear is connected to the swim bladder that amplifies the sound [7]. The ear is also the fish organ for equilibrium [6].

2.2.3 Touch

The salmon has something called ”distant touch“ and this works as a radar system. The salmon detects changes in the water by detecting pressure waves from the environment and from the movement of the own body, with the lateral line, see Figure 3 [8]. This way the salmon can navigate in the dark and when the visibility is very poor. [7]

The salmon is very sensitive to pressure differences in the water, but it is very unsensitive for touch. If the eyes, ears, lateral line, smell or taste do not detect you, you can touch a salmon without it noticing you. Fish are very sensitive to temperature differences and several species can detect temperature differences of 0.05 $^{\circ}$C [6]. [7]

2.2.4 Taste

The taste organs are in the upper part of the mouth and the salmon use it to, according to Grünwald [7], taste food with. According to Erlandson [9] the salmon uses the taste to find the home river when ascending for reproduction.

2.2.5 Smell

The smell organs are located in two openings at the front of the head (nostrils, see Figure 3) and also around the fins. The smell organs are used to find the home river for reproduction. [7]

2.3 Swimming capacity

Fish swimming speed can be categorized in three levels of speed critical for designing fishways:

Cruising A speed that can be maintained for long periods of time (hours)

Sustained A speed that can be maintained for minutes

Burst (or darting) A single effort, not sustainable

It is important that the velocity over the weirs or in the orifices in the fishways do not exceed the burst speed. The velocity in the pools must be less than the sustained speed. The recommended entrance speed for Pacific salmon is 1.2-2.4 m/s. [5]

The swimming speed varies with the length of the fish, the water temperature and with different species. [5]

3 Fishways and fish locks

This chapter will explain the different fishways and fish locks existing today. In fishways, the fish swim up by their own effort and in fish locks and fish elevators the fish is transported or lifted over the obstruction.

3.1 Fish entrance

The most important part of a fishway or fish lock is the entrance. It is important that the fish find the entrance as fast as possible, as the delay causes stress to the fish. Clay [5] states that the entrance to a fishway should be as close as possible to the furthest upstream point the fish reaches by its own effort, and that this is the most overlooked criterium when building a fishway.

There are many ways in which the entrance to the fishway can be easier to find for the fish. One example is to use the spillway to guide the fish to the entrance. Another solution is to use attraction water or auxiliary water at the entrance. Attraction (or auxiliary) water is extra water used at the entrance to create a higher velocity than what the fishway itself can produce.

3.2 Pool type fishway

The pool type fishway is probably the most common type of fishway in the world. In Sweden the most common fishway is the pool and weir type described below [5]. The pool type fishway can be categorized in three different types. The common feature of all pool-type fishways is a number of pools placed after each other with a height difference between the pools. The fish will swim or jump between the pools.

In the weir, or pool and weir type, fishway the connection between the pools (baffles) is in the shape of a weir; see Figure 4(a). In the orifice, or pool and orifice type, fishway, the water does not flow over the baffle, instead the fish uses a submerged orifice to get from one pool to the next (Figure 4(b)). Both weirs and orifices can be used in the same fishway but are still called a weir type; see Figure 4(c).

There are many different designs of the weirs and orifices in pool type fishways. The disadvantage with pool type fishways, and especially the weir type, is the sensitivity to changes in head water. The orifice type fishway is less sensitive to variation in head. The problem with the orifice is that all fishes do not like to swim through them. The best way is to use a combined weir and orifice type, which will yield a fishway not so sensitive to differences in head, and the fish can choose

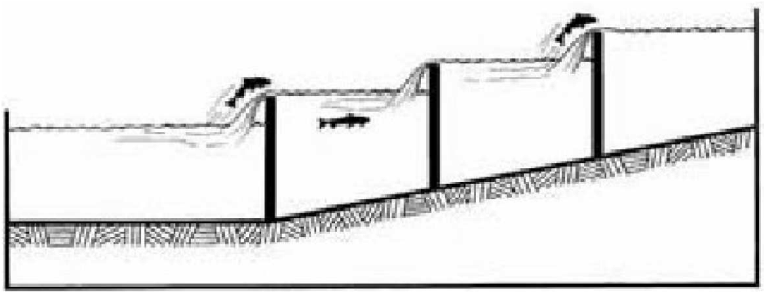

(a) Pool and weir type.

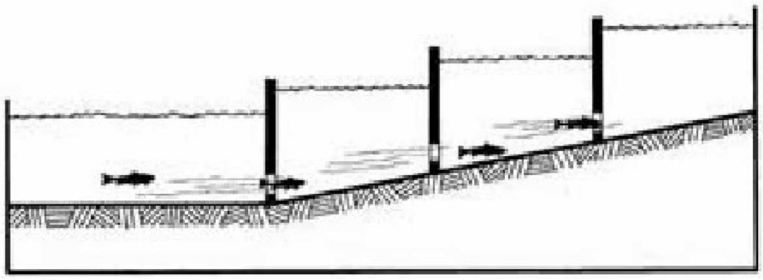

(b) Pool and orifice type.

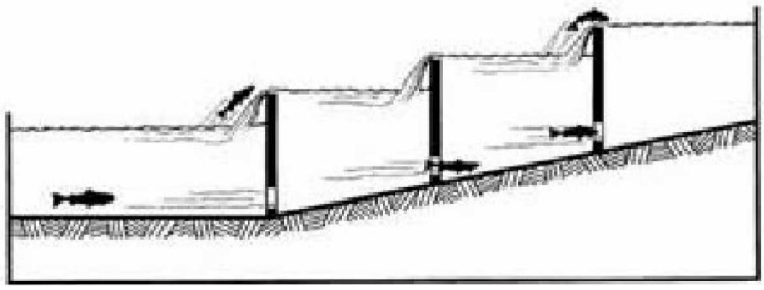

(c) Pool and weir type with both weirs and orifice.

Figure 4: Different types of pool fishways [13].

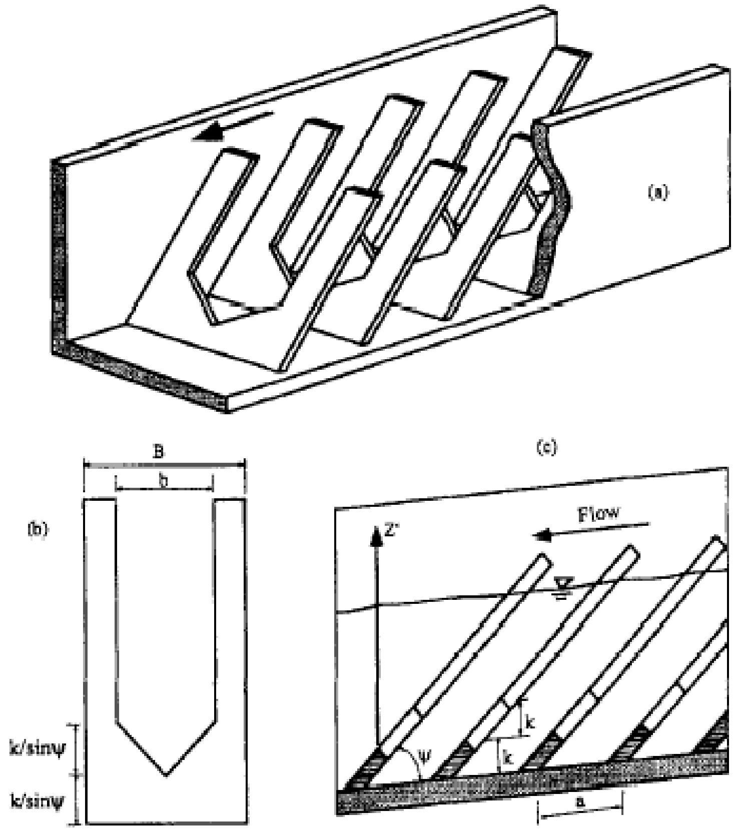

Figure 5: Denil type fishway [15].

between the weir and the orifice. Salmon and trout are thought to use the weir in a fishway but salmon has been seen to use orifice type fishways. [5]

3.3 Denil fishway

The Denil fishway was invented by the fishery scientist Denil in 1908 [5].

The Denil fishway is a rectangular chamber with several baffles at equal distance to each other, with an opening in the middle; see Figure 5. Katopodis et al., [16] describe the so-called standard design of a Denil fishway with the following measures: the chamber has a width of 0.56 m, the central opening is 0.36 m and the distance between the baffles is 0.25 m. The baffles are inclined an angle of 45°. The depth in a Denil fishway is usually 5 times the width of the opening in the baffle (typically 1.8 m). The length and slope of the fishway depends on the

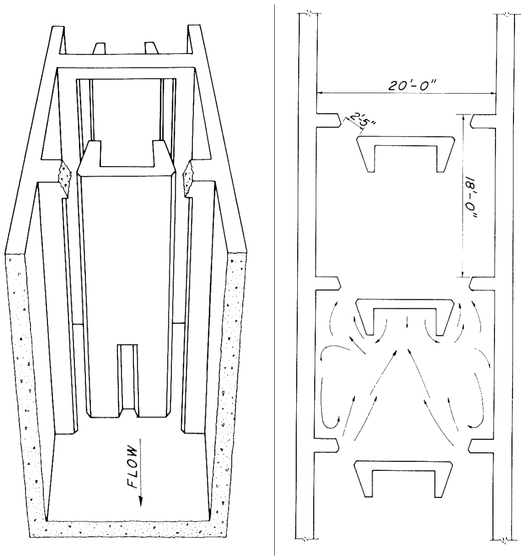

Figure 6: Vertical slot type fishway [5].

capacity of the fish using it, most common is a slope of 10 to 20%, with a length of 5 to 10 m [15]. The goal is for the fish to use its sustained swimming speed through the fishway [5].

The advantage with Denil fishways is that they demand very little maintenance. The disadvantage is that it is very difficult to use auxiliary water and that they use more water than any other type of fishways. [5]

3.4 Vertical slot fishway

The vertical slot fishway, or Hell's Gate type, is of the pool and jet type fishway and looks like a pool and orifice type where the orifice extends over the hole baffle, see Figure 6. The vertical slot fishway works similar as the Denil fishway and they are often used together [5]. The vertical fishway is successfully used to pass salmon and other species in North America and Europe [5].

The advantage with the vertical slot type is that the fish can swim at different depths and it requires little maintenance [5].

3.5 Fish lock

The most common fish lock is the Borland fish lock. The first was constructed in 1949. The lock works by first letting water flow through the fish lock, which

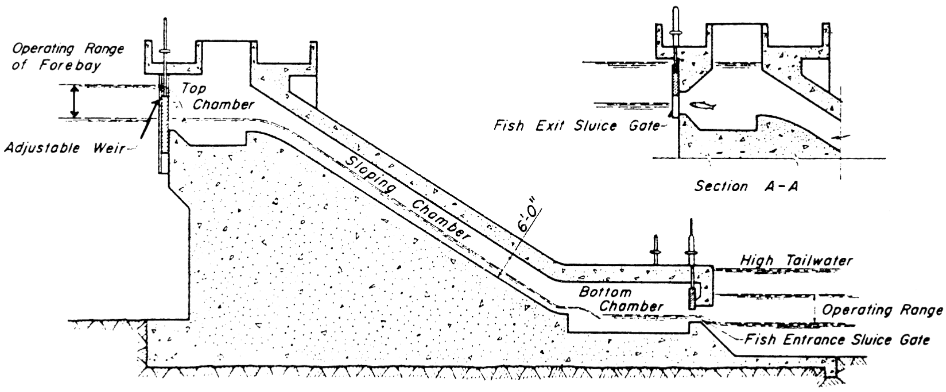

Figure 7: Borland fish lock [5].

attracts fish to swim in to the bottom chamber; see Figure 7. Then the entrance gate closes and water fills the lock. The fish will rise with the water to the top chamber. The last stage is that the entrance gate opens, creating a flow through the lock, and the fish swim out. The Borland lock works in cycles of 1h, 3h etc. The lock is used at dams higher than 10 m. The highest lock in use is 61 m. [5]

The disadvantage with Borland fish lock is that it demands lots of water and that the fish may be injured. If the fish does not swim out of the top chamber in time, it can be hurt by abrasion or impact with the bottom chamber when flushed down the lock as the cycle starts over. The advantage with the Borland fish lock is that it has been successful for descent of smolt and kelt (spent spawners) and also used for eel migration. [5]

The Borland fish lock is best used in small rivers with a small number of migrating fish. [5]

3.6 Fish elevator

Fish elevators are mechanical methods for transporting fish, using e.g. tanks on rails, tank trucks, bucket hung on a cable etc. The fish elevators are often used in rivers with small runs of fish at high dams. The advantage with this method is that it is very flexible. [5]

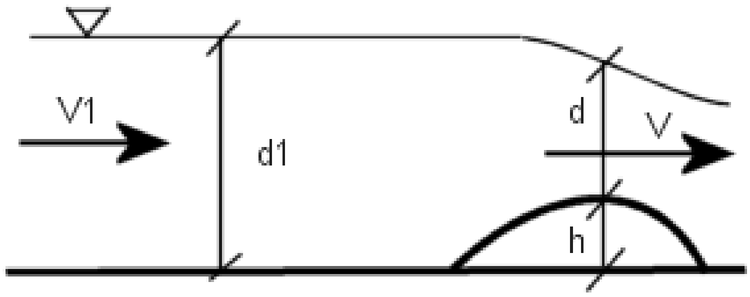

Figure 8: Two dimensional flow over a bump.

4 Theory

To get an idea of how the fish lock will work, the inviscid 2-dimensional theory of flow over a bump is investigated. The theory is then extended to fit the case where the water can flow not only through the lock but also around it.

4.1 Two-dimensional theory

A two-dimensional steady flow of an inviscid incompressible fluid over a bump is considered; see Figure 8. The flow can be described by the Bernoulli equation [17]

$$\frac{\alpha_1 V_1^2}{2g} + d_1 = \frac{\alpha V^2}{2g} + (h + d) \tag{4.1}$$

where α and α_1 are kinetic energy correction factors (see Appendix A.2), V and V_1 are mean velocities (see Appendix A.1), d and d_1 are water depths, h is the height of the bump and g is the acceleration due to gravity. The kinetic energy correction factors are used for compensating for the shape of the velocity profile. If Equation 4.1 is normalized with d_1 and the continuity equation

$$q = V_1 d_1 = V d \tag{4.2}$$

where q is the flow rate per unit width, is used to eliminate V, the equation becomes

$$\frac{\alpha_1 V_1^2}{2gd_1} + 1 - \frac{h}{d_1} = f(d) = \frac{\alpha V_1^2 d_1^2}{2gd_1 d^2} + \frac{d}{d_1}. \tag{4.3}$$

Now the upstream Froude number

$$Fr_1 = \frac{V_1^2}{gd_1} \tag{4.4}$$

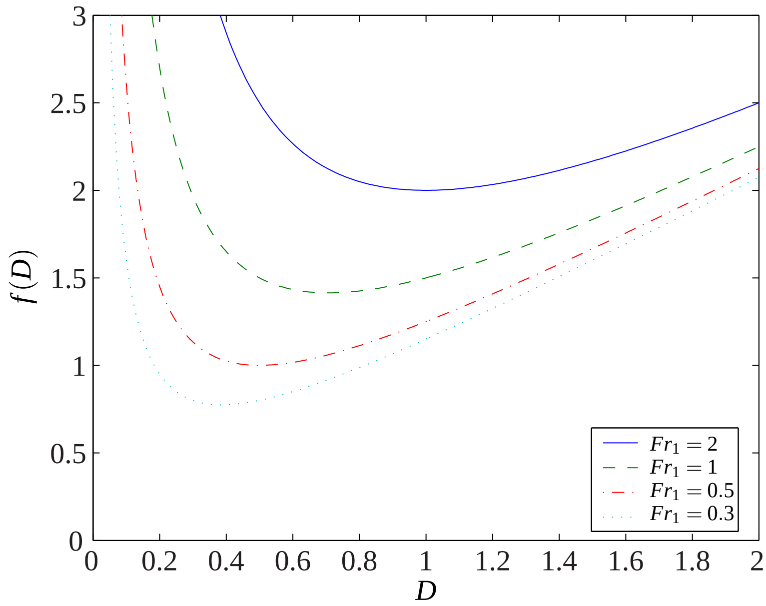

Figure 9: The relation between $f(D)$ and the specific height over the bump at different upstream Froude numbers.

can be introduced in Equation 4.3 together with the dimensionless water depth $D = d/d_1$ over the bump and the dimensionless height of the bump $H = h/d_1$ to get

$$\frac{\alpha_1 Fr_1}{2} + 1 - H = f(D) = \frac{\alpha Fr_1}{2D^2} + D, \tag{4.5}$$

that also can be seen in Figure 9. As seen in Figure 9, there is a minimum f_{min} at, calculated from Equation 4.5,

$$D_* = \frac{d_*}{d_1} = (\alpha Fr_1)^{1/3}. \tag{4.6}$$

At this critical value, the Froude number is unity over the bump

$$Fr = 1 = \frac{V_*^2}{gd_*}. \tag{4.7}$$

By using Equation 4.2 and Equation 4.6, the velocity ratio

$$\frac{V_*}{V_1} = (\alpha Fr_1)^{-1/3}, \tag{4.8}$$

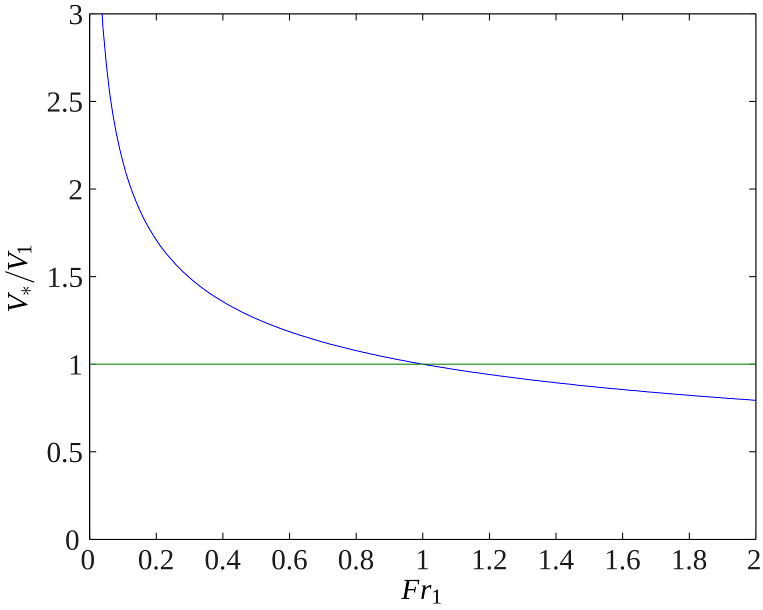

Figure 10: The velocity ratio with respect to the upstream Froude number, with $\alpha = 1$.

can be calculated, to see how much the water velocity over the bump is increased or decreased. The velocity ratio (Equation 4.8) is also displayed in Figure 10 (with $\alpha = 1$), where it can be seen that the upstream Froude number needs to be smaller than unity to get an increased velocity over the bump (i.e. the flow in the lock needs to be subcritical).

The height of the bump that gives critical water velocity over the bump, for a certain upstream Froude number, can be expressed by using Equation 4.5 and Equation 4.6:

$$H_{crit} = 1 + \frac{1}{2}\alpha_1 Fr_1 - \frac{3}{2}\alpha^{1/3} Fr_1^{1/3}. \tag{4.9}$$

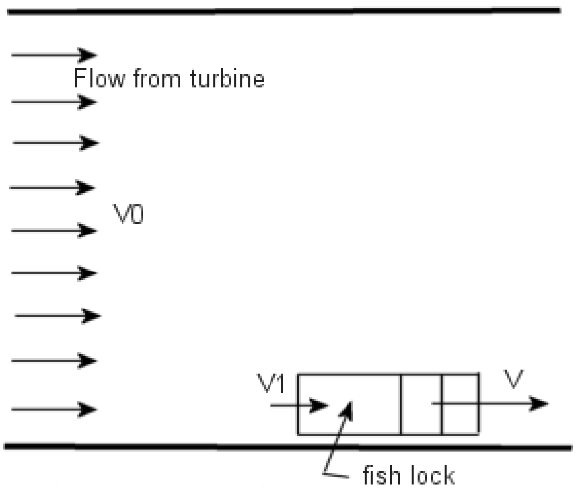

Figure 11: Turbine tailrace with fish lock installed. The water velocity in the tailrace is V_0 and the attraction water velocity is V.

4.2 Extended two-dimensional theory

To know what the actual increase of the velocity will be out of the lock, a model that compares the velocity out of the lock (V) with the velocity of the water around the lock (V_0) (see Figure 11) was made. In the investigation, three cases were considered:

i $H < H_{crit}$

ii $H = H_{crit}$

iii $H > H_{crit}$

For the first two cases, the water is assumed to pass through the lock without any blockage effect. In the third case, the bump is higher than H_{crit} and blockage is assumed to occur in the lock.

Note that the water velocity on the outside of the lock (V_0) is assumed not to change, because the amount of water passing through the lock is very small in comparison to the amount of water passing beside the lock. Hence, the blockage effect of the lock will not contribute to a significantly higher velocity of the water.

If the bump is lower than the critical height ($H < H_{crit}$), no blockage will occur and the velocity in the lock will be the same as that outside of the lock ($V_1 = V_0$). The velocity ratio can be calculated directly from Equation 4.2 and 4.5.

In the second case the bump height equals the critical bump height ($H = H_{crit}$), i.e. the flow over the bump is critical. No blockage will occur and the velocity in the lock will be the same as that outside of the lock ($V_1 = V_0$). The maximum increase in velocity will be, according to Equation 4.8

$$\frac{V}{V_0} = \frac{V}{V_1} = \alpha^{-1/3} Fr_1^{-1/3}. \tag{4.10}$$

In the third case the bump height is larger than the critical bump height ($H > H_{crit}$), and blockage will occur. The velocity in the lock will be lower than outside of the lock ($V_1 < V_0$), but the velocity over the bump will remain critical and the upstream water depth (d_1) will remain the same. In the classic theory, where all the water passes over the bump, this bump height would lead to damming of the upstream water level. The increase in velocity will now be according to Equation 4.8

$$\frac{V}{V_0} = \frac{V}{V_1}\frac{V_1}{V_0} = \alpha^{-1/3} Fr_1^{-1/3} \frac{V_1}{\sqrt{gd_1}} \frac{\sqrt{gd_1}}{V_0}. \tag{4.11}$$

If the upstream Froude number based on the velocity outside the lock is introduced as

$$Fr_0 = \frac{V_0^2}{gd_1}, \tag{4.12}$$

the velocity increase (Equation 4.11) can be written as

$$\frac{V}{V_0} = \alpha^{-1/3} Fr_1^{-1/3} \frac{Fr_1^{1/2}}{Fr_0^{1/2}} = \alpha^{-1/3} \frac{Fr_1^{1/6}}{Fr_0^{1/2}}. \tag{4.13}$$

If the velocity increase (V/V_0) is used as a function of H (using Equation 4.5) and Fr_0, the velocity increase can be calculated with a known height of the bump and the velocity of the water around the lock; Figure 12.

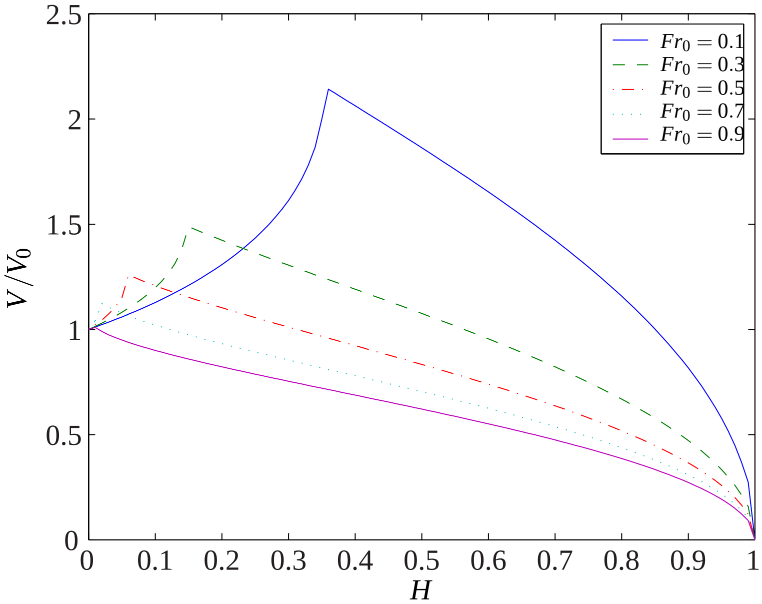

Figure 12: Velocity increase (V/V_0) as a function of bump height (H) at different Froude numbers based on the velocity outside the lock (Fr_0).

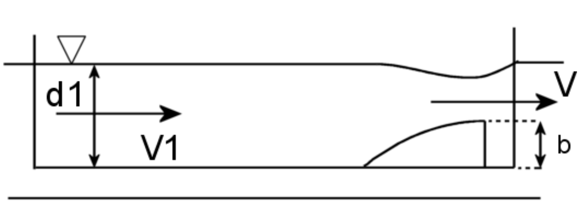

(a) Fish lock with bump.

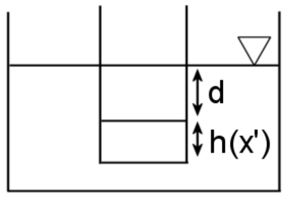

(b) Cross section of flume and fish lock.

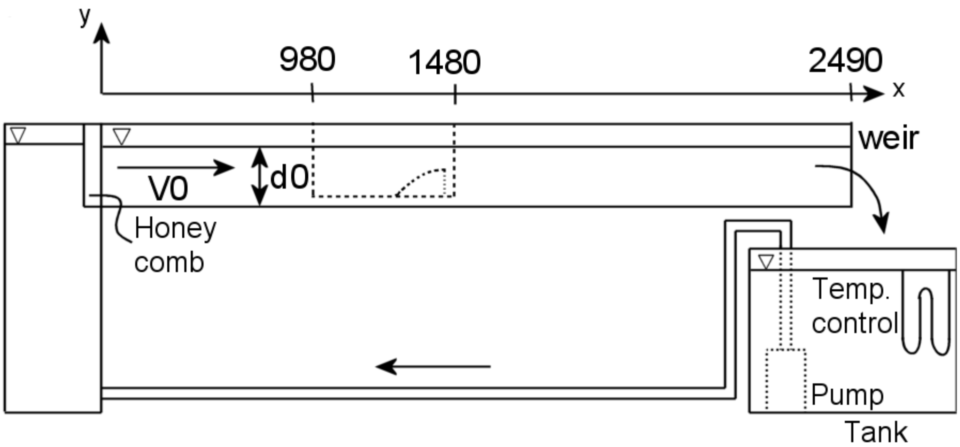

(c) Experimental setup of water flume with fish lock.

Figure 13: Experimental setup of water flume. All dimensions in mm.

5 Experimental setup

The method used to study this problem was to make a model of the fish lock and experimentally study the flow in it. The lock was partly submerged in a water flume representing the turbine tailrace. To study the behavior, laser Doppler velocimetry (LDV) was used to measure the velocity distribution in the water.

5.1 Water flume

The water flume is a 2490 mm long horizontal open channel of 10 mm Plexiglas with a inner cross section of 200 $\times$ 300 mm; see Figure 13. At the inlet of the flume, there is a honey comb to provide a more uniform velocity distribution. The honey comb is 75 mm thick and the holes have a diameter of 7.6 mm. At the outlet of the flume there is a V-notch weir to control the flow rate, see section 5.2.1. The system was driven by a pump at the flow rate of 5.3 $\times 10^{-3}$ m^3/s ($\pm$1%) during the

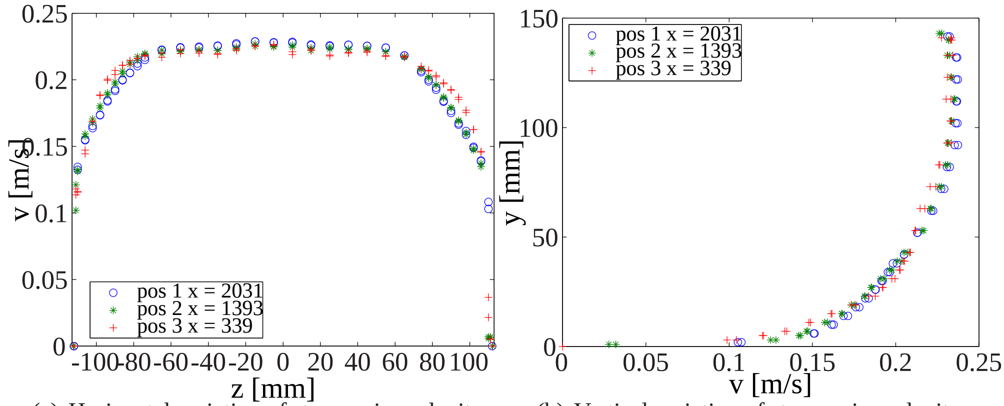

(a) Horizontal variation of streamwise velocity. (b) Vertical variation of streamwise velocity.

Figure 14: Velocity distribution in the water flume, with no fish lock installed. Measurements taken at three different positions.

tests. The water depth, d_0, was 118 ± 1 mm at x = 2078 mm and the Reynolds number in the flume was Re=$U \times d_0/\nu \approx 18000$.

To investigate how the velocity profiles developed in the flume, and where the best place would be to place the lock, the initial flow field (the flow field in the flume with no lock in it) was mapped using LDV. The velocity profiles were taken in three sections of the flume, position one at x = 2031 mm, position two at x = 1393 mm and position three at x = 339 mm. The flow rate was maximum of what the pump could produce (8.1 dm^3/s) with the Coriolis mass flowmeter connected to the system. The measurements were taken in one horizontal (Figure 14(a)) and one vertical (Figure 14(b)) direction, like a cross. Each profile was measured twice to check the repeatability of the measurements.

In Figure 14, it can be seen that the velocity profiles are similar along the flume with fairly thick boundary layers. From these measurements it was decided to place the lock in the middle of the flume (around z = 0) at a distance of 3 cm above the bottom to avoid the major boundary layer effects; see Figure 13(b).

5.1.1 The fish lock

The model of the fish lock is a 500 mm long open channel made of 1.7 mm window glass, see Figure 13(a). The inner cross section of the lock is 200×96 mm. In the lock, different bumps were placed made of Styrofoam with a plastic film glued to the top, to create a smooth surface. The bumps were modeled with a quadratic polynomial, so the bumps could easily be scaled with the bump height. The shape of the bump is given by

$$h(x') = b - \frac{x'^2}{12b} \; (x' \geq 0, h \geq 0) \tag{5.1}$$

where b is the maximum height of the bump. The bump is cut off at $x' = 0$ (Figure 13(a)), creating a steep end at the downstream end and a smooth slope at the upstream end. The bump heights were 22, 34, 47, 70 and 80 mm. The bump was placed 40 mm from the outlet of the lock, to be able to measure the velocity over the bump using LDV.

5.2 Instrumentation

5.2.1 V-notch weir

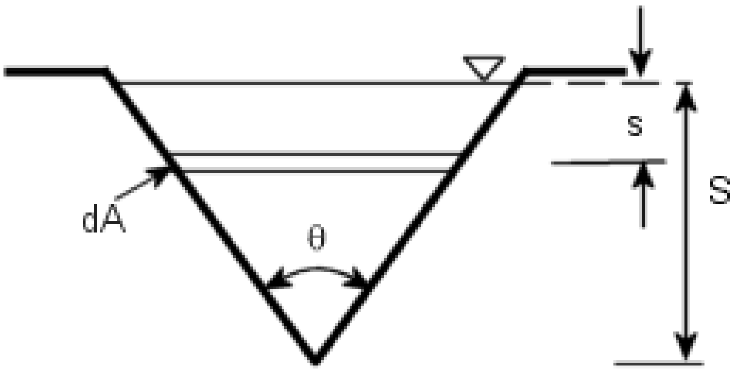

Figure 15: V-notch weir.

To measure the flow rate in the flume a V-notch weir was used; see Figure 15. The weir is used to measure the flow rate in the flume by measuring the height of the water, S, over the weir.

Finnemore and Franzini (2002) show by using the flow rate $dQ = \sqrt{2gs}dA$ of the discharge through an area $dA = 2xds$, where $x = (S-s)tan(\theta/2)$, that the flow over the weir is

$$Q = \mu\frac{8}{15}\sqrt{2g}tan\frac{\theta}{2}S^{5/2} = \mu K_0 S^{2.5} \tag{5.2}$$

where μ is a correction factor. The weir was calibrated with a mass flowmeter; see section 5.2.3. The correction factor was determined to $\mu = 0.74$; see Figure 16. The height of the water over the weir was measured with a caliper.

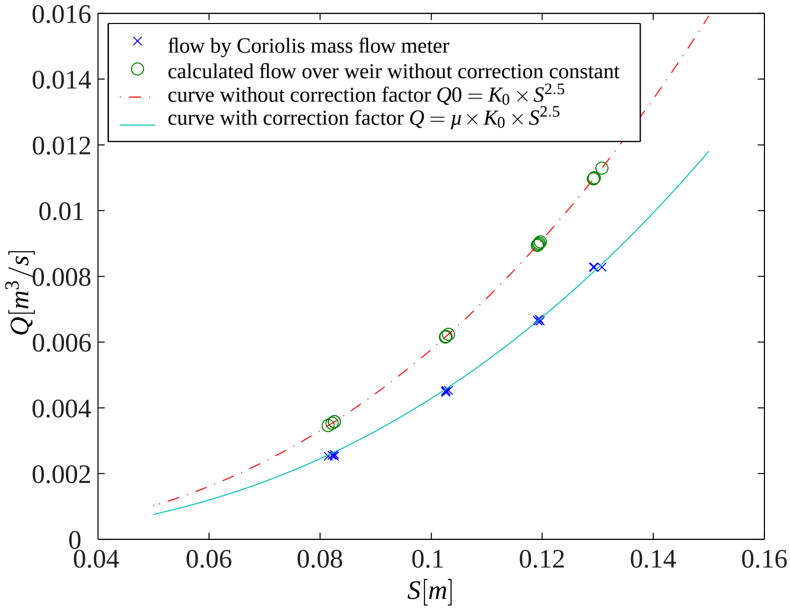

Figure 16: Calibration of the flow rate over a V-notch weir. The solid line represents the calibrated flow with a correction factor of $\mu = 0.74$.

5.2.2 Control of temperature

The water in the system is heated mainly by the pump. During the measurements, the water temperature needs to be controlled, since the temperature has a large effect on the characteristics of the water. The water temperature in the flume was controlled with a cooling system to a temperature of 22.1 $\pm$ 0.2 °C. In Figure 17, measurements of the temperature with respect to time at a constant flow rate is shown. In the figure, it can be seen that the system heats the water with 2.7°C/h with the pump running at maximum effect.

Temperature was measured with the mass flowmeter, using its built-in thermometer.

The cooling system used to control the temperature was placed in the water tank, where the pump, that creates most of the heat, also was located, see Figure 13(c).

5.2.3 Mass flowmeter

A mass flowmeter measures the mass flow rate of a fluid. The Coriolis mass flowmeter used here consists of a vibrating U-shaped pipe in which the fluid flows.

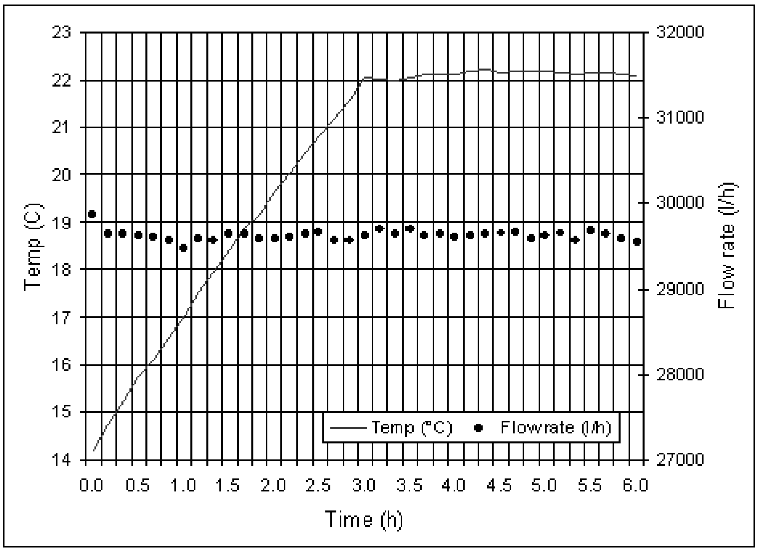

Figure 17: Measurements of the temperature in the flume with temperature control installed in the system (temperature set to 22.1°C).

The pipe is set to vibrate at its natural frequency which is inversely proportional to the square root of the pipe's mass. By knowing the natural frequency of an empty pipe or a pipe filled with a fluid of known density, the density of a unknown fluid can be determined by measuring the change in natural frequency. [18]

The flow of the fluid through the vibrating pipe makes the pipe twist and the force acting on the pipe is directly proportional to the mass flow, which will be the same for the twist amplitude, due to the Coriolis effect. The error in mass flowmeters is usually under 0.5 %. [18]

The mass flowmeter used in this project is a Danfoss MassFlo coriolis flowmeter with an error of 0.5% . The mass flowmeter was connected to the system to calibrate the V-notch weir and also to monitor the temperature control. The mass flowmeter was connected to the system directly after the pump when it was used. During the measurements with the fish lock the mass flowmeter was disconnected from the system, to allow a higher flow rate.

5.2.4 Laser Doppler velocimetry

Laser-Doppler velocimety or LDV is a non-intrusive point measuring method for measuring velocities in fluids. The fact that the LDV measures velocities in a point gives the technique good resolution in time but bad resolution in space.

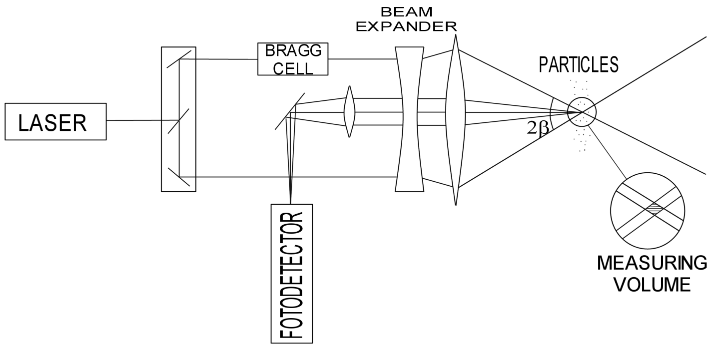

Figure 18: Schematic figure of backward scatter LDV setup.

The LDV technique is based on the doppler shift in the reflecting light from moving particles in a fluid. The velocity of the particle is proportional to the frequency shift, which means that the velocity of the particle can be determined only from the geometry of the setup and the wave length of the light, i.e. no calibration is needed. The particles in the fluid need to follow the fluid successfully in order to represent the velocity of the fluid. The wave length of the light should be of the same order as the diameter of the particles in the fluid. The diameter of the particles is usually around 1 μm, so visible light can be used ($0.45-0.7\mu m$). Even ultraviolet light can be used, but setting up an optical system with non-visible light is much harder. In theory, LDV is able to measure velocities from 0.01 mm/s to 10^6 m/s. The advantage with LDV is that it is a non-intrusive method (apart from the particles) and it is not sensitive to the temperature or the compound of the fluid. The disadvantage with LDV is that the medium must be transparent and the experimental setup must allow optical access. [18]

When measuring with one light source and one detector the ratio between the doppler frequency and the reference frequency becomes

$$\frac{\omega_D}{\omega_0} = 2\sin(\gamma/2)\frac{U}{c} \tag{5.3}$$

where ω_D is the Doppler frequency, ω_0 is the reference frequency, 2γ is the angle between the incoming light and the reflected light, U is the velocity of the particle and c is the speed of light. If a velocity of 1 m/s is measured with this method the ratio ω_D/ω_0 must be determined with a resolution of 10^{-10} in order to get a accuracy of 1 %. This is not possible with the techniques available to day.[18]

To be able to measure the Doppler shift, two light beams are used. The two light beams are directed at the measuring volume, with the angle 2β, see Figure 18.

The scattered light is detected with one detector in one direction (it is also possible to use one light beam and two detectors). Because the light hits the particle at different angles the reflected light from the two beams will have slightly different frequencies. If the frequencies from the two light beams are compared the result is

$$\omega_{s2} - \omega_{s1} = 4\pi \frac{U_x}{\lambda} \sin(\beta) \tag{5.4}$$

where $\omega_{s1} = \omega_{01} + \omega_{D1}$ is the reference frequency plus the Doppler frequency for the first beam, $\omega_{s2} = \omega_{02} + \omega_{D2}$ is the reference frequency plus the Doppler frequency for the second beam, U_x is the velocity of the particle and λ is the wave length of the light. The difference between the frequencies is in the order of the velocity divided by the wave length of the light and this frequency is easier to detect. Now the velocity of the particle can be determined but the direction, if the particle is moving forward or backward through the measuring volume, is still unknown. This problem can be solved by shifting the frequency of one of the beams, typically by 10-80 MHz. The direction can now be determined; if the resulting frequency is lower than the shifted frequency the particles are moving in one direction and if the resulting frequency is higher than the shifted frequency the particles are moving in the opposite direction. This is practically done by letting one of the beams pass an opto-acoustic modulator e.g. a Bragg-cell (see Figure 18). [18]

The velocities in the flume and lock were measured using laser Doppler velocimetry. The system is a two component setup from Dantec with an 85 mm fiber optic probe. The two component setup uses two different wave lengths, 514.5 nm and 488 nm. Two component system means that the velocities can be measured in two directions, in this case perpendicular to each other. It is possible to measure three directions with LDV, but this demands a second probe. When measuring in three directions many complicating factors arise. The problems mainly arise from the fact that the measuring volumes are not orthogonal [19]. The system in this case uses only one probe for both components and the beams are located so one of them is measuring the streamwise velocity component and the other measuring the vertical velocity component in the water. A beam expander (1.98) was fitted to the probe to reduce the measuring volume. The focal length of the front lens was 310 mm and the resulting measuring volume was 0.076×0.838 mm for the streamwise velocity component (514.5 nm) and 0.072×0.761 mm for the vertical velocity component (488 nm). The probe is fitted to a three-coordinate traverse system controlled by Dantec's BSAFlow software v.2 on a PC, that also controls the signal conditioning hardware. The seeding used in the water was polyamide particles with a mean diameter of 5 μm (Dantec's PSP-5). The system operated in backscatter mode, which means that the reflecting light from the particles is collected with the same probe that the beams are emitted from. The hardware operated in non-coincident burst mode (spectrum analysis method).

5.3 Errors

Uncertainty in the measurements originates from the experimental setup and the measurement system. The setup has been carefully designed to yield stable experimental conditions. The measurement uncertainty is composed of uncertainty due to bias errors and precision errors. LDV measurements are associated with a variety of bias errors, such as error in the calibration factor, velocity bias, validation bias, angular bias and probe alignment/configuration bias. The system was setup to minimize the different bias errors.

The velocity bias is due to the fact that the particle rate through the measuring volume is related to the flow velocity, leading to a bias towards a higher velocity [19]. The bias was compensated for by weighting each velocity sample with its residence time in the measuring volume.

The precision error was estimated by a repeatability test. Each profile was measured twice and the standard deviation of each pair of measurements was estimated to yield a 95% confidence interval. The overall accuracy of the velocity measurements was $\pm 5\%$, with locally larger errors close to the walls and the free surface.

5.4 Measuring procedure

Due to LDV being a pointwise measuring technique it needs to be traversed, and the velocities measured in specific points. Measuring points at the fish lock outlet were taken over the bump along a vertical line in the middle of the lock from the top of the bump to the water surface at x = 1440 mm (see Figure 13). At the same position along the x-axis, data on the outside of the lock was collected from the bottom of the flume to the surface (between the lock and the flume wall) and under the lock along a vertical line in the middle of the flume. Measurements at the inlet of the lock were taken 48 mm from the inlet, inside the lock at x = 1028 mm. Measurements were also taken along a horizontal line from the flume wall and through the lock, both at the inlet and at the outlet. Approximately 55 points total were acquired in random order for each bump.

The sample time in each measuring point was determined by testing different sample times. Sixteen measuring points were measured in the lock vertically from the bottom of the lock to the surface of the water, with different sample times. Each profile was measured five times with each sample time. The times tested were 60, 90, 180, 360 and 450 s. The mean velocity for each measuring point at each sample time were calculated and the velocities were compared with the mean. The criterium for a good sample time was an error of $\pm1\%$ in the lock with no bump. The sample time was set to 90 s. The second criterium for the measurements was to have at least 10,000 samples in each measuring point. This resulted in sample times between 90 and 4500 s.

6 Results and discussion

Results from the measurements are shown in Figure 19.

The velocity outside the lock, when there is no bump in the lock, is used as reference for measuring the velocity ratio over the different bumps. In the full scale test, the lock will only represent a small fraction of the total cross sectional area and the change in flow rate through the lock will not affect the velocity outside the lock significantly.

In Figure 19, it is seen that the velocity on the outside of the lock ($\diamond$) is higher for the locks with bumps than for the measurements with no bump, due to the blockage effect by the lock that forces more water to the outside of the lock. The velocity at the upstream end of the lock ($+$) also shows the blockage effect. The velocity is much lower for the 80 mm bump compared with the velocity for b = 0 mm. The upstream velocity is used to calculate Fr_1, which can be used to theoretically calculate the height of the bump that gives critical flow over the bump.

The speed over the bump is the accelerated flow that the fish will be attracted to. As seen in Figure 19, the velocity for the 80 mm bump is significantly higher than the velocity on the outside of the lock for measurements with no bump, which indicates that the fish lock may produce an attractive flow for the fish.

In Figure 19 it can also be seen that the velocity under the lock does not change much for different bump heights.

For every bump, the critical height H_{crit} of the bump based on the upstream Froude number, was calculated. Figure 20 shows that H_{crit} increases as Fr_1 decreases with larger bump heights B, until critical flow is reached ($Fr = 1$). This is the point where damming of the upstream water surface would occur, if the flow could only pass over the bump. However, here the flow will be forced to the outside of the fish lock with maintained surface level upstream. An increase of the bump height at this point would decrease the flow rate through the fish lock. Even though the local acceleration would still increase, the overall acceleration would not. The maximum speed increase was 40% for b = 80 mm (Figure 20).

The flow in the lock can be qualitatively described using the 2-d inviscid energy equation. The extended 2-d theory does not describe the flow in and around the lock well, see Figure 21. It can be seen that the calculated velocity increase is over estimated. In the extended 2-d theory the blockage in the lock would appear first when the flow over the bump was critical. In the measurements the blockage effect in the fish lock is present in all the measurements. This depends on the friction in the lock, which is not accounted for in the 2-d theory.

The blockage effect caused by the fish lock's friction is partly due to the low Reynolds number in the model experiment. This effect will be smaller in the full-scale test, where the lock, and thus the Reynolds number, will be larger and the effect from the boundary layers will be smaller.

A small amount of damming occurs upstream the fish lock due to the blockage effect, which will counteract the deceleration inside the lock. This effect is considered small in the model test and will be insignificant in the full-scale test.

In the full-scale test, it is important to take into consideration the water depth over the bump. If the fish are to swim into the lock there must be a certain minimum water depth at the inlet. If the fish are to jump into the lock no such consideration needs to be accounted for. It is reported that some salmon uses the orifice in pool fishways [5], so it is possible that some salmon rather swim in to the lock than jump.

By placing the lock in the turbine tail race it is possible to reduce the stress on the fish. Clay [5] says that the entrance to a fishway should be as close as possible to the furthest point upstream the fish reaches by its own effort, as it is important that the fish find the fishway as fast as possible in order to reduce the stress on the fish. By placing the fish lock in the turbine tail race, it would not be the furthest point upstream the fish reaches, but it would be were the fish first try to ascend before trying the fishway located at the dam. The fish would pass the dam faster than if they were using the fishway at the dam, thus reducing the stress on the fish.

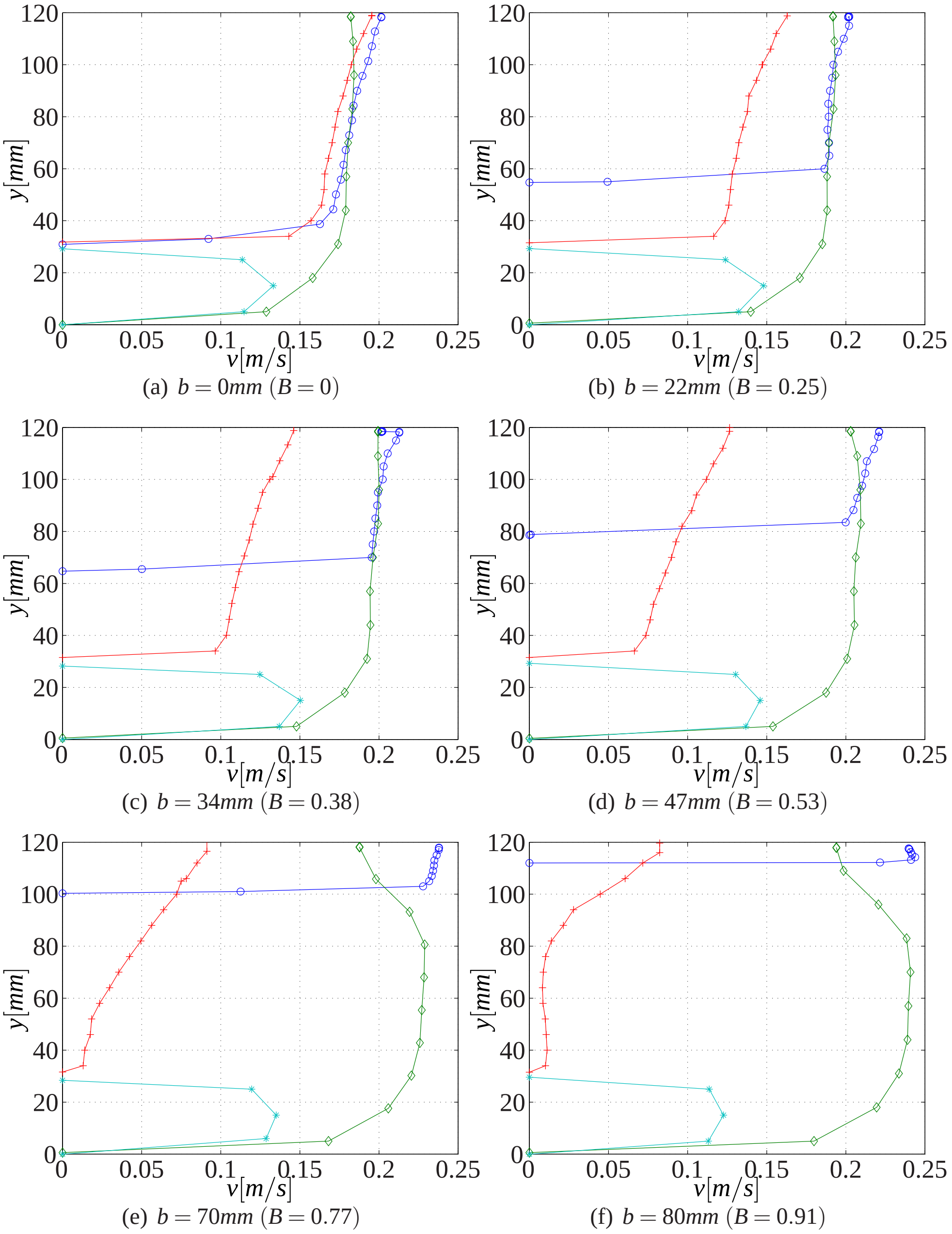

(a) $b = 0mm$ $(B = 0)$

(b) $b = 22mm$ $(B = 0.25)$

(c) $b = 34mm$ $(B = 0.38)$

(d) $b = 47mm$ $(B = 0.53)$

(e) $b = 70mm$ $(B = 0.77)$

(f) $b = 80mm$ $(B = 0.91)$

Figure 19: The horizontal velocity component with different bumps. Here b is the highest point on the bump and $B = b/d_1$ is the dimensionless highest point. The symbols denote the following velocity profiles:
$\circ$: velocity over the bump $\diamond$: velocity outside the lock
$+$: velocity at the inlet of the lock $*$: velocity under the lock.

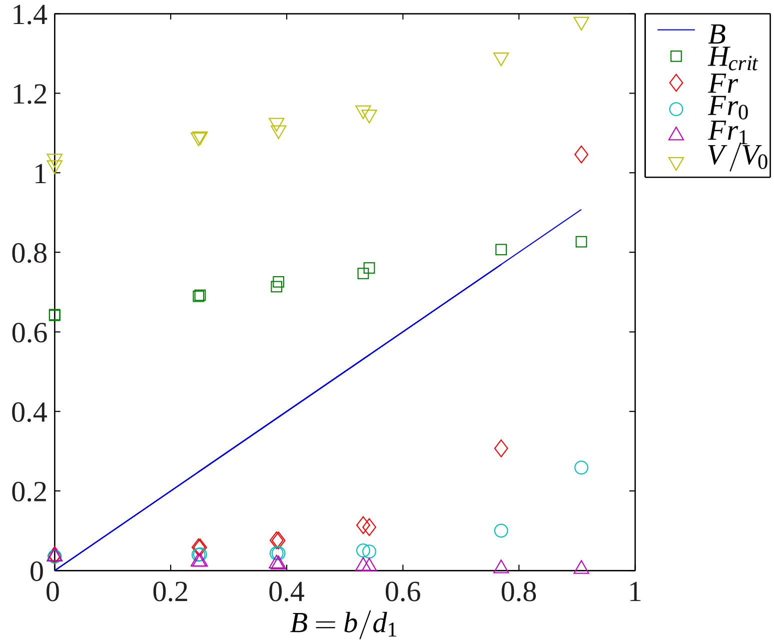

Figure 20: Results of different non dimensional factors.

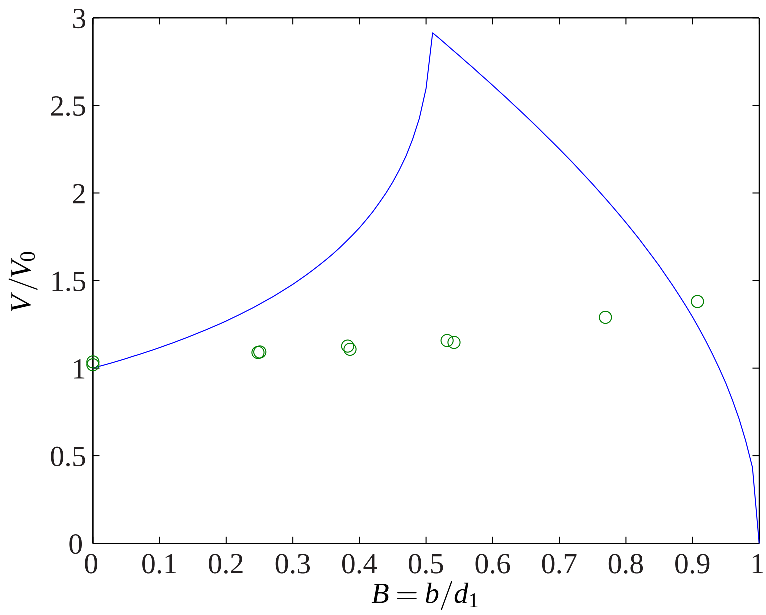

Figure 21: Results from calculations (solid lines) and experiment (points) with $Fr_0 = 0.04$ *based on the velocity outside the lock with no bump.*

7 Conclusions

A model test of a new type of fish lock has been performed. Critical flow was reached over the bump and a significant acceleration of the flow was accomplished. Scale up effects are thought to improve the performance of the fish lock.

The two-dimensional theory used to describe the flow over-estimated the acceleration of the water, due to fact that the friction wasn't accounted for in the theoretical model.

By placing the fish lock in the turbine tail race it is possible to reduce the stress on the fish.

8 Future work

In the summer of 2004 a full-scale prototype of the fish lock will be tested at the Sikfors hydropower plant (40 MW) in the Pite river in Sweden. A smaller prototype of the lock will also be tested on parr salmon at Hedens fishfarm in Boden, Sweden.

Further measurements on the accelerated water after the lock is planned in the lab setup to see how far behind the lock the accelerated water can be detected.

Calculations on the lock needs to be improved, the friction needs to be accounted for in the theory.

The shape of the bump can be optimized after what the fish likes.

References

[1] Lawrence K. Forbes and Leonard W. Schwartz. Free-surface flow over a semicircular obstruction. *J. Fluid Mech.*, 114:299–314, 1982.

[2] Jean-Marc Vanden-Broeck. Free-surface flow over an obstruction in a channel. *Phys. Fluids*, 30(8):2315–2317, August 1987.

[3] M. S. Faltas, S.N. Hanna, and M. B. Abd el Malek. Linearised solution of a free-surface flow over a trapezoidal obstacle. *Acta Mech.*, 78(3-4):219–233, 1989.

[4] S. N. Hanna. Free-surface flow over a polygonal and smooth topography. *Acta Mech.*, 100(3-4):241–251, 1993.

[5] Charles H. Clay. *Design of Fishways and Other Fish Facilities*. Lewis publishers, second edition, 1995.

[6] Nils E Eriksson & Gunnar Johnson. *Fisken*. LTs fölag, 1978.

[7] Jan Grünwald. *Konsten att fiska lax*. Norstedts Förlag AB, 1992.

[8] Jens Meulengracht-Madsen. *Fiskars beteende*. LTs förlag, 1967.

[9] Erik Erlandson. *Lax & havsöring*. Naturia Förlag AB, 1988.

[10] Benny Lindgren. *Där laxen vandrar*. Settern, 1991.

[11] http://www.washingtontourist.com/salmon/journey/two.html, 040518.

[12] http://www.flyfishusa.com/flies/fry.htm, 040518.

[13] Erik Degerman et al. *Ekologisk fiskevård*. Sportfiskarna, 1998.

[14] http://www.geocities.com/athens/atrium/5924/fishanatomy.htm, 040518.

[15] Rajaratnam et al. Hydraulics of resting pools for denil fishways. *Journal of Hydraulic Engineering*, pages 632–638, July 1997.

[16] Katopodis et al. Denil fishways of varying geometry. *Journal of Hydraulic Engineering*, pages 624–631, July 1997.

[17] E. J. Finnemore & J. B. Franzini. *Fluid mechanics with engineering applications*. McGraw-Hill, Boston, 2002.

[18] Arne V. Johansson and P. Henrik Alfredsson. Experimentella metoder inom strmningsmekaniken. Institutionen för Mekanik, KTH, Stockholm, 1988.

[19] N. Damaschke H.-E. Albrecht, M. Borys and C. Tropea. *Laser Doppler and Phase Doppler Measurement Techniques*. Springer, 2003.

Nomenclature

α	Kinetic energy correction factor for velocity profile over the bump	
α_1	Kinetic energy correction factor for velocity profile at the inlet of the lock	
β	Angle between the light beams in a LDV setup	[rad]
γ	Angle between incoming light beam and reflected light when measuring with one light source and one detector	[rad]
λ	Wave length	[m]
μ	Correction factor for V-notch weir	
ω_0	Reference frequency (frequency of measuring light beam)	[Hz]
ω_D	Doppler frequency	[Hz]
ω_{s1}	Reference frequency for the first light beam in an LDV setup	[Hz]
ω_{s2}	Reference frequency for the second light beam in an LDV setup	[Hz]
θ	Angle of the V-notch weir	[rad]
B	Dimensionless highest point on the bump	
b	Highest point on the bump	[m]
c	Speed of light	[m/s]
D	Dimensionless water depth over the bump	
d	Water depth over the bump	[m]
D_*	Dimensionless water depth over the bump at critical flow	
d_*	Water depth over the bump at critical flow	[m]
d_1	Water depth at the inlet of the lock	[m]
Fr	Froude number over the bump	
Fr_0	Froude number based on the velocity outside the lock and the water depth at the inlet of the lock, d_1	
Fr_1	Froude number at the inlet of the lock	

g	Acceleration due to gravity	[m/s^2]
H	Dimensionless height of the bump	
h	Local bump height	[m]
H_{crit}	Dimensionless bump height at critical flow	
Q	Flow rate	[m^3/s]
q	Flow rate per unit width	[m^2/s]
S	Water depth in V-noth weir	[m]
U	Velocity of a single particle	[m/s]
U_x	Velocity of a particle in the x-direction	[m/s]
V	Mean velocity over the bump	[m/s]
V_*	Mean velocity over the bump at critical flow	[m/s]
V_0	Mean velocity outside the lock	[m]
V_1	Mean velocity at the inlet of the lock	[m/s]

Glossary

alevin	Newly hatched salmon living on the nutriment in the yolk sac.
anadromous	A fish that reproduce in fresh water and live the rest of its life in salt water.
burst or dart speed	The top speed for the salmon.
cruising speed	A speed that the salmon can maintain for long periods of time (hours).
degree-days	The mean temperature in Celsius in a day multiplied with the number of days.
eyed-out	The eyes of the fetus is visible through the egg.
fishway	A devise to help a fish pass obstructions in a river, where the fish swim up by their own effort
fry	Young salmon, see also alevin, parr and smolt.
kelt	A salmon that have spawned.
lateral line	A line along the salmon body that detect small pressure variations in the water.
parr	Fry living in the river feeding on small animals in the water.
postsmolt	Smolt in the sea, until the length of 25 cm.
redd	The nest in which the eggs are laid.
smolt	Fry ready for life in the sea.
smoltification	When the parr becomes smolt.
spawn	To bring forth a new generation of salmon.
sustained speed	A speed that the salmon can maintain for minutes.
swim bladder	A sac inside the salmon's body by which the fish can control buoyancy.
yolk sac	Nourishment in a food sac attached to the alevin.

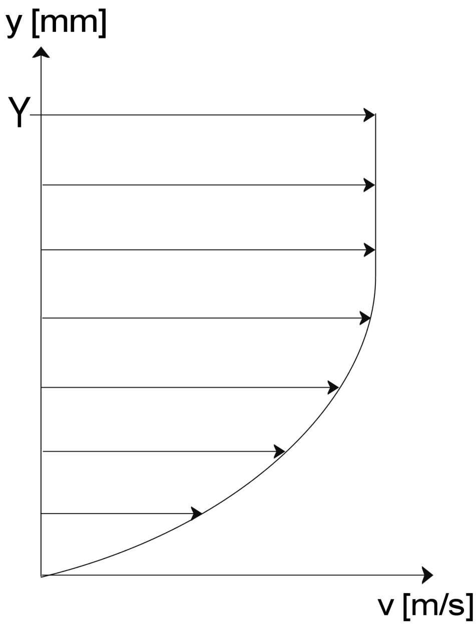

Figure 22: 2-dimensional velocity profile.

A Method of calculation

A.1 Mean velocity

The method for calculating the mean velocity of a velocity profile (Figure 22)was [17]

$$V = \frac{1}{Y} \int_0^Y v(y) dy. \tag{A.1}$$

A.2 Kinetic energy correction factor

The kinetic energy correction factor is used to express the true value of the kinetic energy when mean velocities are used. The method for calculating the kinetic energy correction factor was [17]

$$\alpha = \frac{1}{YV^3} \int_0^Y v^3(y) dy. \tag{A.2}$$